

# The role of reticular chemistry in the design of CO<sub>2</sub> reduction catalysts

Christian S. Diercks<sup>1,2,3</sup>, Yuzhong Liu<sup>1,2,3</sup>, Kyle E. Cordova<sup>1,2,3,4</sup>  and Omar M. Yaghi<sup>1,2,3,4\*</sup> 

**The problem with current state-of-the-art catalysts for CO<sub>2</sub> photo- or electroreduction is rooted in the notion that no single system can independently control, and thus optimize, the interplay between activity, selectivity and efficiency. At its core, reticular chemistry is recognized for its ability to control, with atomic precision, the chemical and structural features (activity and selectivity) as well as the output optoelectronic properties (efficiency) of porous, crystalline materials. The molecular building blocks that are in a reticular chemist's toolbox are chosen in such a way that the structures are rationally designed, framework chemistry is performed to integrate catalytically active components, and the manner in which these building blocks are connected endows the material with the desired optoelectronic properties. The fact that these aspects can be fine-tuned independently lends credence to the prospect of reticular chemistry contributing to the design of next-generation CO<sub>2</sub> reduction catalysts.**

The grand challenge in photo- and electrocatalytic carbon dioxide reduction to value-added carbon products lies in the fact that a single catalytic system must control the interplay between efficiency, activity and selectivity (Fig. 1). In this context, the efficiency governs the energy cost of the process and is defined by a material's optical (photocatalytic systems) and/or electronic (photo- and electrocatalytic systems) properties. When considering the optical properties, one must engineer the material's bandgap to enhance the photon efficiency, while the electronic properties are related to the inherent charge carrier mobility, both of which impact the quantum and Faradaic efficiencies, respectively. The activity provides the turnover and yield and is related to the number of and the diffusion to the active sites. These directly correlate to the surface area and metrics of the catalyst structure. Finally, the selectivity dictates the desired product and purity thereof and is directly linked to the chemical nature of the catalyst with both the binding affinity to CO<sub>2</sub> and the redox behaviour of the active site playing pivotal roles. Thus far, a number of different catalytic systems have been discovered (albeit to a certain extent serendipitously) for effectively catalysing the reduction of CO<sub>2</sub>; however, there remains a noticeable absence of a consummate solution that combines all of these properties together in one material.

Much of what has been done synthetically has been inspired by what is accomplished in natural photosynthesis<sup>1–3</sup>. Nature has evolved catalysts with perfected activity and selectivity for CO<sub>2</sub> reduction; however, the efficiency of the system is not very high. The fact that efficiency is low appears counterintuitive at first, but can be understood when considering the conditions under which the reaction takes place. Due to the low concentration of CO<sub>2</sub> in the atmosphere, relative to this process, the rate-determining step is carbon fixation. The problem then lies with the fact that there are more photons absorbed than can be used for affecting carbon conversion, with the remaining energy dissipated to feed other processes. Simply put, nature affords a highly active and selective system, but one lacking optimal efficiency for carbon conversion (Fig. 1).

The first class of synthetic materials developed — metals and metal oxides (heterogeneous catalysts)<sup>4,5</sup> — were targeted for their optoelectronic properties, which held promise for improving the efficiency problem inherent to nature. Not only were these materials able to achieve superior efficiency, but their activity was also demonstrated as being amenable to fine-tuning through size and morphology control<sup>6,7</sup> (Fig. 1). In this way, materials increase their surface area, thus effectively improving their activity, while at the same time altering their optoelectronic properties. It would be preferable to control each of these independently. Another aspect of heterogeneous inorganic catalysis that must be put forth is the fact that these materials are difficult to rationally control on the molecular level and the most active systems rely mainly on the use of precious metals<sup>8</sup>. Even with such drawbacks, inorganic materials remain at the forefront in performance for both photo- and electrocatalytic CO<sub>2</sub> reduction<sup>6,9</sup>. The next class of synthetic materials — molecular (homogeneous) catalysts<sup>10–12</sup> — by virtue of the nature of the organic ligand, can be tailored towards enhanced selectivity and, to a certain extent, efficiency (Fig. 1). Although the molecular nature of this class of materials provides a handle over these two characteristics, it often comes at the expense of activity. This is primarily due to catalyst deactivation (for example, dimerization) and limitations with respect to solubility of the catalyst as well as the substrate. Furthermore, activity is hindered in molecular systems because they require multiple components that are at the mercy of randomness in solution. In order to address these activity issues, one must be able to effectively orient the multiple components in an ordered manner such that they operate synergistically. The question then arises: how do we combine the advantages of each class of material in one system? Ideally, this system must be an extended (heterogeneous) structure with an ordered and metrically defined organic backbone capable of being tailored to achieve the appropriate optoelectronic properties. In this way, the material can achieve optimal efficiency, activity and selectivity in such a way that they are not mutually exclusive, but rather mutually beneficial<sup>13</sup>.

<sup>1</sup>Department of Chemistry, University of California, Berkeley, California, USA. <sup>2</sup>Kavli Energy NanoScience Institute at Berkeley, Berkeley, California, USA.

<sup>3</sup>Berkeley Global Science Institute, University of California, Berkeley, California, USA. <sup>4</sup>Center for Research Excellence in Nanotechnology, King Fahd University of Petroleum and Minerals, Dhahran, Saudi Arabia. \*e-mail: [yaghi@berkeley.edu](mailto:yaghi@berkeley.edu)

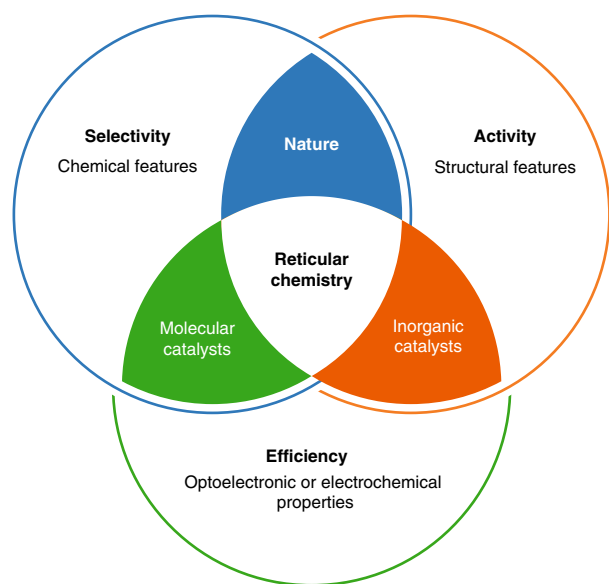


**Fig. 1 | The grand challenge in developing CO<sub>2</sub> reduction catalysts lies in the interplay between selectivity, activity and efficiency.** Selectivity is governed by chemical features, such as binding affinity, redox properties and acid/base character. Activity is founded on structural and material properties like surface area, crystallinity and particle size. Finally, efficiency is defined by the optoelectronic properties (that is, photonic, quantum and Faradaic efficiencies, as well as the morphology). In this context, nature provides highly active and selective catalysts, but lacks optimal efficiency. In contrast, inorganic catalysts, such as metals and metal oxides, display high efficiency and activity. However, tuning the selectivity at the molecular level remains difficult. Homogeneous molecular catalysts are capable of achieving high selectivity and efficiency, but are inherently limited with regard to activity. The prospect of realizing all three aspects in a single system may only be achieved by reticular chemistry.

Metal–organic frameworks (MOFs) and covalent organic frameworks (COFs) — reticular materials — represent ideal platforms for realizing this in one system<sup>14,15</sup>. In terms of selectivity, these materials are constructed from molecular building units, which allow for the integration of well-defined, highly selective molecular catalysts within the backbone of the architecture<sup>16,17</sup>. With respect to activity, both are well-known for their high surface areas and tunable pore metrics, thus allowing for facile diffusion of substrates to the active sites<sup>18,19</sup>. Finally, in the context of efficiency, great strides have been made in engineering the bandgaps and/or intrinsic charge carrier mobility of different MOF/COF structures<sup>20,21</sup>. The important aspect to remember here is that one is not limited by structure type — the right framework can be chosen in terms of chemical composition, pore metrics and optoelectronic properties, all the while allowing for the addition of the appropriate metal catalyst. The MOF/COF backbone is responsible for activity and efficiency and the framework chemistry of the structure is responsible for the selectivity. Indeed, these can all be optimized independently (Fig. 1). In a sense, these classes of materials can be considered ‘materials on demand’, as critically assessed here.

### MOF photocatalysts for CO<sub>2</sub> reduction

**First generation: selectivity and activity.** Molecular CO<sub>2</sub> reduction catalysts are highly selective, but lack the efficiency and activity necessary for practical use<sup>22</sup>. A strategy to take advantage of their selectivity, while at the same time enhancing their activity, is to spatially isolate them to prevent catalyst poisoning by dimerization. To accomplish this, molecular catalysts can be grafted onto a solid

support, and MOFs are ideal platforms for three reasons: (i) they are often transparent single crystals, which allows for light to penetrate through the whole material, in contrast to amorphous solids or powders, which suffer from light scattering; (ii) the high surface area of MOFs and related materials is an advantage as it maximizes the areal density of active sites; and (iii) the fact that MOFs can be considered as pores without walls allows for easy access of the substrate to those active sites.

**Site isolation.** The first MOF, a modified version of UiO-67, capable of reducing CO<sub>2</sub> was reported in 2011<sup>23</sup>. The synthetic strategy for developing this MOF was to integrate a well-known molecular catalyst into the backbone of the framework. Re<sup>I</sup>(bpy)(CO)<sub>3</sub>Cl (bpy = 2,2'-bipyridine) has been extensively studied as a molecular CO<sub>2</sub> reduction catalyst in homogeneous systems<sup>24,25</sup>. While this molecular catalyst is initially very selective and active, it quickly degrades due to off-pathway dimerization. By employing Re<sup>I</sup>(dcbpy)(CO)<sub>3</sub>Cl (dcbpy = 2,2'-bipyridine-5,5'-dicarboxylic acid) as an organic linker in an isorecticular functionalized UiO-67 framework, the catalytic centres become site-isolated, which prevents degradation by dimerization<sup>23,26</sup> (Fig. 2a). The Re<sup>I</sup>(dcbpy)(CO)<sub>3</sub>Cl functionalized UiO-67 photocatalyses CO<sub>2</sub> reduction towards CO in an acetonitrile solution with trimethylamine serving as a sacrificial reducing agent. The resulting turnover number (TON) was 10.9 over the course of 20 h — a result that is almost threefold higher than that of the homogeneous Re<sup>I</sup>(dcbpy)(CO)<sub>3</sub>Cl linker. It is noted, however, that the recovered functionalized UiO-67 solid was inactive for further CO generation. This is attributed to carbonyl moieties detaching from the rhenium centre on the MOF backbone during the catalytic cycle, as evidenced by the loss of CO stretching vibrations.

**Open metal sites.** There are considerable synthetic challenges associated with integrating homogeneous molecular photocatalysts within a MOF. To overcome this challenge and still maintain the high selectivity previously achieved, attention turned to exploring MOFs that are composed of redox active metals and available coordination sites within their secondary building units (SBUs), such as MIL-101(Fe) (ref<sup>27</sup>). This MOF's Fe<sub>3</sub>O SBUs have up to three possible open coordination sites (terminal water ligands cap the clusters) that are capable of effectively adsorbing and subsequently reducing CO<sub>2</sub>. Under visible light irradiation and with triethanolamine (TEOA) as a sacrificial agent, MIL-101(Fe) was shown to reduce CO<sub>2</sub> exclusively to formate with a TON of 1.2 over 24 h. Electron spin resonance spectroscopy studies revealed that photogenerated Fe<sup>II</sup> was directly involved in the reduction process. Furthermore, MIL-101(Fe) was shown to significantly outperform other Fe-based MOFs, MIL-53(Fe) and MIL-88B(Fe) (refs<sup>28,29</sup>) due to its open metal sites.

**Second generation: optical efficiency.** Generally, the catalytic sites do not absorb light in the visible region; a requirement for maximizing photonic efficiency. The bandgap can be engineered through tailoring the MOF backbone to ensure that the frameworks' optical properties match the proper range of light absorption. The efficiency of MOFs can be optimized in the following ways: (i) organic functionalization aimed at integrating chromophoric antennae into the framework<sup>30,31</sup>; (ii) inorganic modification through the judicious choice of metal character and cluster size of the SBUs<sup>32</sup> (it is noted here that the SBU can be considered as discrete metal oxide nanoparticles linked together through organic linkers); and (iii) incident light can be intensified locally by wrapping MOF structures around plasmonic nanoparticles.

**Bandgap engineering.** Ti<sup>IV</sup>-based MOFs combine the photocatalytic activity of titanium oxide with the light absorption properties of organic linkers. This combination affords materials that are

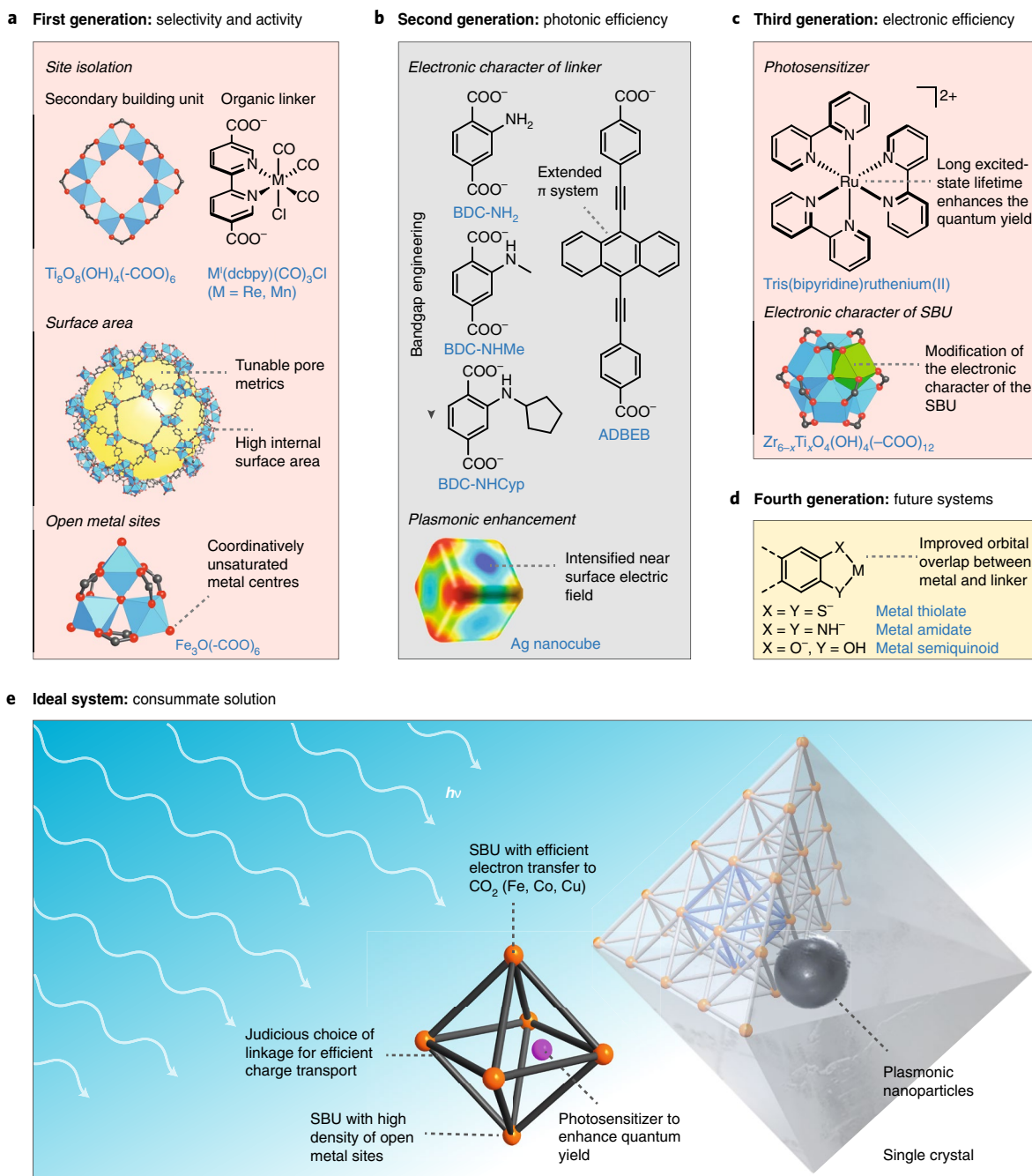


**Fig. 2 | The design of MOFs as CO<sub>2</sub> reduction photocatalysts.** The modular nature of MOFs allows for precise control over the installation of various chemical and structural features in order to enhance selectivity, activity and efficiency. **a**, The first generation of MOF photocatalysts increased selectivity through site isolation (discrete nanoparticle metal oxide SBUs, site isolated molecular catalysts) and enhanced their activity by tailoring the pore metrics and surface area. **b**, In the second generation, the photonic efficiency was optimized by altering the nature of the linker (bandgap engineering through functionalization and conjugation of the linker) and by integration of plasmonic nanoparticles to expose the catalyst to their intensified near surface electric field. **c**, The third generation optimized the electronic efficiency through molecular photosensitizers to improve the apparent quantum yield or by tuning the electronic character of the SBU to improve charge separation and to slow down the recombination rate of photogenerated electron-hole pairs. **d**, The fourth generation — future systems — must further enhance the electronic efficiency by improving charge carrier mobility, which will yield higher quantum efficiency. **e**, The ideal MOF system must build on and combine the success of the previous generations.

photocatalytically active under ultraviolet (UV)–visible light<sup>33</sup>. MIL-125(Ti) has an absorption band edge at 350 nm allowing photocatalysis to take place in the UV region. Using sunlight to reduce CO<sub>2</sub> directly would be ideal; however, the majority of sunlight is in the visible range — too low in energy to induce photoreduction within such systems. Toward this end, an isoreticular functionalized analogue, termed NH<sub>2</sub>-MIL-125(Ti), was synthesized bearing amino

functionalities on the linker<sup>34,35</sup>. The resulting MOF adsorbed visible light with the band edge extending to ~550 nm. The photocatalytic reduction of CO<sub>2</sub> was then performed in acetonitrile with TEOA as the sacrificial agent under visible light irradiation. Over the course of 10 h, NH<sub>2</sub>-MIL-125(Ti) afforded 8.14 μmol of formate. The fact that the unfunctionalized MIL-125(Ti) did not show any photocatalytic activity under these conditions demonstrates the need for the

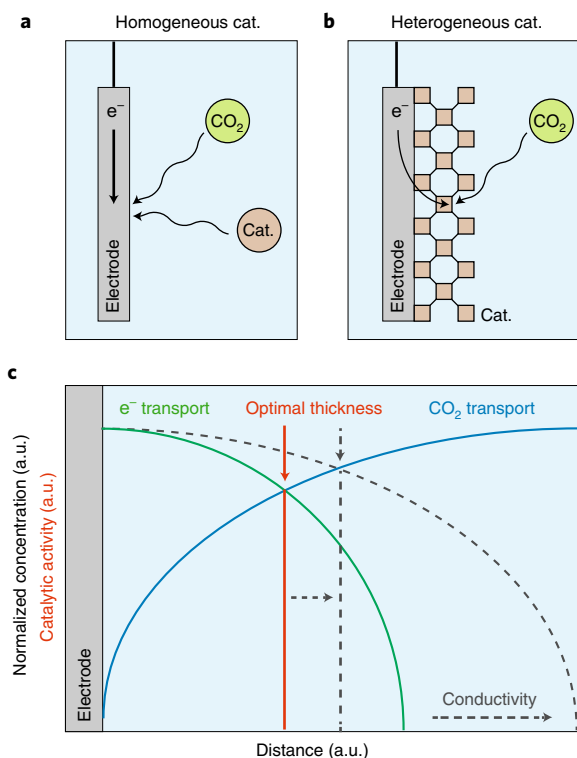


**Fig. 3 | Conceptual principles for developing MOFs/COFs as electrochemical CO<sub>2</sub> reduction catalysts.** **a**, In electrocatalytic CO<sub>2</sub> reduction, the activity of homogeneous molecular catalysts is intrinsically limited by the necessity for concurrent migration of both CO<sub>2</sub> and the catalyst to the electrode in order to affect transformation. As such, the reaction is at the mercy of random molecular fluctuations in solution. **b**, In contrast, heterogeneous catalysts can effectively be interfaced with the electrode material, and thus the only limiting factor for turnover is the diffusion of CO<sub>2</sub> to the active sites. **c**, With respect to efficiency, electrocatalysts need to balance the interplay between electron and mass transport. A given material has an optimal catalyst thickness, which maximizes the reciprocity of these two intrinsic material characteristics.

amino functionality on the linker of NH<sub>2</sub>-MIL-125(Ti) in order to obtain photocatalytic activity. Given the pronounced effect of linker substitution on catalytic activity, an isorecticular series of MOFs was designed where the amino functionality of the original NH<sub>2</sub>-MIL-125(Ti) was replaced with *N*-alkyl groups of varying connectivity (primary and secondary *N*-alkyl amines) and chain length<sup>36</sup>. This series exhibits reduced optical bandgaps, which are directly related to the inductive donor ability of the alkyl substituents. In addition, the secondary *N*-alkyl functionalized MOFs feature larger apparent quantum yields than the primary *N*-alkyl derivatives, owing to an increase in their excited-state lifetime. The highest efficiency of this series, NHCyp-MIL-125(Ti) (Cyp = cyclopentyl), is substantially enhanced due to a smaller bandgap, a longer excited-state lifetime, and a resulting improved apparent quantum yield ( $E_g = 2.30$  eV,  $\tau = 68.8$  ns,  $\Phi_{app} = 1.80\%$ ) compared to the parent NH<sub>2</sub>-MIL-125(Ti) ( $E_g = 2.56$  eV,  $\tau = 12.8$  ns,  $\Phi_{app} = 0.31\%$ ).

**Plasmonic enhancement.** For most MOF photocatalysts, a second component, either a photosensitizer or a co-catalyst, is needed to achieve a significant TON for CO<sub>2</sub> reduction. Here, inefficient electron transfer between the molecular photosensitizer and the MOF catalyst, as well as slow mass transport of the homogeneous component through the framework channels, are detrimental to the activity of the catalyst. To further optimize the performance, all

components of the catalytic system must be integrated within one single material<sup>37,38</sup>. Re<sub>3</sub>-MOF (UiO-67, 3 Re centres incorporated on the linker) was coated onto Ag nanocubes (Ag ⊂ Re<sub>3</sub>-MOF), which spatially confines photoactive Re centres to their intensified near-surface electric fields. This composite material resulted in a sevenfold enhancement of CO<sub>2</sub>-to-CO conversion (compared to the molecular catalyst) under visible light with long-term stability maintained up to 48 h (TON = 2.9)<sup>39</sup>.

**Third generation: electronic efficiency.** A standing challenge for increasing efficiency lies in the fact that not every photon absorbed by the system is productively used for photocatalysis. Upon absorption of light, photons can be either emitted or excited electrons are transferred to the substrate. It is necessary to consider how a material's electronic properties can be designed to ensure that the lifetime of charge-separated states is long enough for electrons to be transferred to the CO<sub>2</sub> substrate to affect the chemical transformation. Two approaches have been utilized in MOF photocatalysts: (i) introducing a molecular photosensitizer within the MOF system (not grafted) — here, the photosensitizer is a molecular complex that has visible light absorption, inherent high quantum efficiency, and acts as a mediator to prolong the charge-separated state lifetime; and (ii) altering the electronic character of the inorganic SBU. In this scenario, by changing the nature of the metal, the excited-state lifetime can be extended. A longer lifetime leads to a higher quantum efficiency and higher catalytic activity.

**Photosensitizer.** An important factor for the low efficiency of the aforementioned catalysts is the low apparent quantum yield of these systems. To address this shortcoming a manganese bipyridine complex, Mn(dcbpy)(CO)<sub>3</sub>Br, was incorporated into UiO-67 and the reaction carried out in conjunction with [Ru(dmb)<sub>3</sub>]<sup>2+</sup> (dmb = 4,4'-dimethyl-2,2'-bipyridine) as a photosensitizer<sup>40,41</sup>. In DMF/TEOA and in the presence of 1-benzyl-1,4-dihydronicotinamide as a sacrificial donor, this system efficiently catalyses CO<sub>2</sub> reduction to formate under visible light irradiation. Over the course of 18 h the catalyst reaches a TON of 110. Owing to the use of the photosensitizer, the high quantum yield of  $\Phi_{formate} = 13.8\%$  in the visible region of the spectrum is far superior to those of previously reported MOF systems. The catalyst can be reused over several cycles, although its photochemical performance does decrease due to a loss of the photosensitizer after prolonged irradiation to visible light.

**Electronic character of the SBU.** Photosensitizers have a problem of reusability and they function as an added component to the catalytic system. In this regard, altering the electronic character of the SBU of a MOF catalyst is seen as a viable alternative approach. One such example is that of post-synthetically modifying the Zr<sub>6</sub>O<sub>4</sub>(OH)<sub>4</sub> SBU of UiO-66 with catalytically active Ti<sup>IV</sup> (ref. 42). On its own, the SBU of UiO-66 cannot accept electrons from the linker due to a mismatch in the redox potential energy levels of the SBU and the linker. However, by doping the SBU of UiO-66 with Ti<sup>IV</sup> ions, in conjunction with tuning the light absorption properties of the linker, a new material was created. Through a combination of diffuse reflectance UV-visible, photoluminescence, and UV light photoelectron spectroscopy measurements this material was shown to: (i) supply an added light absorption route; (ii) generate electron-hole pairs; (iii) effectively slow the recombination rate of those photogenerated electron-hole pairs; and (iv) improve charge separation. The photocatalytic reduction of CO<sub>2</sub> to formic acid was performed under visible light in an acetonitrile, TEOA (sacrificial base), and 1-benzyl-1,4-dihydronicotinamide (sacrificial reductant) suspension. The mixed-metal MOF achieved an average TON of ~6 over 6 h with 13 electrons being transferred from each incorporated Ti<sup>IV</sup> site.

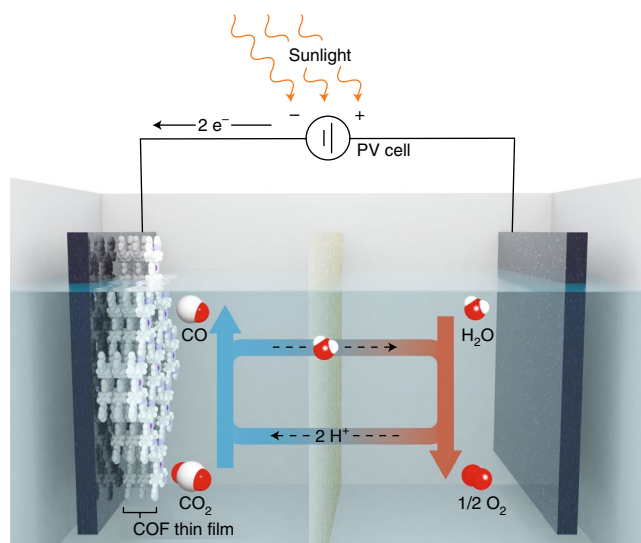


**Fig. 4 | Schematic of the proposed photoelectrocatalytic reduction of CO<sub>2</sub> to CO by COF-366(Co) in a hypothetical photoelectrochemical cell.** Photoelectrochemical reduction of carbon dioxide combines the advantages of both the photocatalytic and electrocatalytic approaches. Similar to photocatalysis, this setup makes use of sunlight as the energy source. The fact that the reaction is carried out in two half cells, as in the electrocatalytic conversion, circumvents the need for the addition of a sacrificial donor because electrons are generated from the oxidation of water on the counter electrode. Atom colours: C, grey; H, white; N, blue; and Co, purple.

**Fourth generation: future systems.** Taking stock of these advances, the fourth generation MOF photocatalyst quickly takes shape (Fig. 2). In this future system, a high density of open metal sites, functioning as the active sites, are needed. The metals must be chosen judiciously (for example, Fe, Co or Cu) in order to allow for efficient electron transfer to adsorbed CO<sub>2</sub> substrates. This takes care of the activity and selectivity challenges. To also ensure high optical efficiency, the MOF backbone must be appropriately conjugated and functionalized to absorb visible light. The MOF backbone must also have high charge carrier mobility by choosing coordinating groups that ensure proper frontier orbital overlap and redox matching between the organic linker and the SBU (for example, metal–semiquinoid, metal–dithiolene and diiminobenzosemiquinonate)<sup>43–45</sup>. Strategies to achieve this have focused on incorporating linker and metal mixed valency to increase the charge density<sup>20,46</sup>. For future systems, not all of these components are equal in terms of importance. In practice, the rate-limiting structural feature, which has plagued other photocatalytic systems, remains charge carrier recombination<sup>47</sup>. These last two aspects have yet to be fully addressed in MOFs<sup>48,49</sup>.

### MOF and COF electrocatalysts for CO<sub>2</sub> reduction

In order to operate, photocatalytic processes are inherently at the mercy of sunlight (that is, quantum efficiency). This means that sunlight dictates the voltage that can be used to affect CO<sub>2</sub> reduction. With too little sunlight, efficiency drops significantly. Furthermore, photogenerated electron flux is generally lower than electron flux provided by an external electrical source under an applied potential. Additionally, due to the fact that sunlight contains photons of multiple wavelengths, varying potentials are generated. This is disadvantageous since the applied potential exponentially correlates to the current density of product formation and thus varying potentials lead to decreased figures of merit. To avoid this, electrocatalysis is an attractive alternative process because one does not have to rely

on the constant presence of sunlight as an energy source and one can dial in the exact voltage needed to ensure selectivity towards a desired product.

**First generation: selectivity and activity.** Homogeneous catalysts have been optimized for high selectivity toward CO<sub>2</sub> reduction; however, they lack sufficient activity. The three key considerations for ensuring that an electrocatalyst maintains the high selectivity observed in homogeneous catalysts, but also achieves high activity are: (i) incorporate homogeneous catalysts within the backbone of an extended framework<sup>50,51</sup>; (ii) the reaction must take place in an aqueous media because at room temperature CO<sub>2</sub> has a higher solubility than in organic solvents. Furthermore, water as a reaction medium is beneficial as it facilitates proton and electron transfer processes (that is, increases the activity)<sup>52</sup>; and (iii) there needs to be a controlled interface between the catalyst and the electrode. The reason for this is to favour a two-component over a three-component system (Fig. 3a,b). If no permanent interface exists, the catalyst, CO<sub>2</sub>, and the electrode must come together at the exact same time to carry out the reaction (three-component system). When the catalyst is interfaced with the electrode, one effectively removes a variable from this equation (two-component system).

**Maximizing areal density.** MOF-525(Fe) consists of metalloporphyrin linkers, which serve as active sites<sup>53</sup>. Thin films of this MOF were electrophoretically deposited on an electrode in order to maximize the areal density of the active sites while achieving the necessary electronic contact with the electrode<sup>54</sup>. Electrolysis at an overpotential of ~650 mV was carried out in a tetrabutylammonium hexafluorophosphate/DMF electrolyte solution resulting in 15.3 μmol cm<sup>-2</sup> and 14.9 μmol cm<sup>-2</sup> of CO and H<sub>2</sub>, respectively. When taking into account the amount of electronically accessible catalyst, these values translate into a turnover frequency (TOF) for CO formation of 64 h<sup>-1</sup> and a TON of 272. The addition of a weak Brønsted acid, 2,2,2-trifluoroethanol, increased the CO production by sevenfold with the TON reaching 1,520 after 3.2 h. Mechanistic studies on the catalytic activity of MOF-525(Fe) showed that in this system the turnover is limited by electron transport.

**Second generation: efficiency.** Thin films of MOFs allow for the necessary electronic contact of the catalytic material with the electrode. The first generation of MOF catalysts is, however, limited in regard to their charge carrier mobility properties. It is therefore necessary to further assess the impact of mass transport in the system. This is rooted in the fact that to improve efficiency one must balance both mass and electron transport (Fig. 3c), such that a system does not have to solely rely on one property over the other.

In the realm of porous materials, the diffusion of CO<sub>2</sub> to the catalytic sites causes the local concentration of CO<sub>2</sub> close to the electrode to decrease with increasing film thickness. Consequently, the number of active sites that are exposed to a high concentration of CO<sub>2</sub> is limited. There are two tunable parameters for maximizing the efficiency of such systems: (i) fine-tuning of the thickness to the point in which the interplay between electron and mass transport is optimized; and (ii) enhancing the charge carrier mobility of the material to allow for efficient electron transport to active sites further away from the electrode. The first point is related to engineering the morphology of the catalyst and the second point entails modifying the inherent electronic properties of the material.

**Matching electron and mass transport.** An aluminium porphyrin-based MOF<sup>55</sup>, Al<sub>2</sub>(OH)<sub>2</sub>TCPP-Co [TCPP-H<sub>2</sub> = 4,4',4'',4'''-(porphyrin-5,10,15,20-tetrayl)tetrabenzoate], comprising cobalt porphyrin active sites was employed for the electrocatalytic reduction

of CO<sub>2</sub> to CO (ref. 56). Here, thin films of the MOF were directly grown on a conductive carbon disk electrode. The synthetic strategy is based on the formation of aluminium oxide thin films, serving as metal precursors, via atomic layer deposition (ALD). Subsequent MOF formation was carried out by reacting the coated electrode with the linker under solvothermal conditions. This strategy holds great promise for balancing electron and mass transport as the thickness of the precursor can easily be controlled by the number of ALD cycles, which was found to be proportional to the thickness of the resulting MOF thin films. As such, the thickness of the aluminium oxide precursor was varied by changing the number of ALD cycles from 5 to 100 resulting in aluminium oxide films of 0.5 to ~10 nm. The performance of the resulting MOF catalyst initially improves with increasing film thickness until reaching a maximum of ~2.8 mA cm<sup>-2</sup> at 50 ALD cycles. This translates to a MOF thickness of ~30–70 nm. The fact that the performance decreases at a higher thin film thickness demonstrates that the optimal thickness was achieved. The optimized catalyst thickness exhibited a Faradaic efficiency for CO production of up to 76% and, within 7 h, reached a turnover number of 1,400.

**Enhancing the charge carrier mobility.** In comparison to MOF systems, layered imine-based COFs are attractive due to their superior charge carrier mobility. COF-366, another material comprising porphyrin building blocks, was reported to have a high charge carrier mobility of 8.1 cm<sup>2</sup> V<sup>-1</sup> s<sup>-1</sup> (ref. 57). As a result, a metalated COF-366, termed COF-366-Co, and derivatives thereof were investigated as electrocatalytic CO<sub>2</sub> reduction catalysts<sup>58</sup>. COF-366-Co was demonstrated to reduce CO<sub>2</sub> in water at an overpotential of -0.55 V, producing 36 mL mg<sup>-1</sup> of CO over the course of 24 h with a Faradaic efficiency of 90%. Interestingly, increasing the pore size of COF-366-Co, by means of isorecticular expansion (1.8 to 2.3 nm), to realize COF-367-Co had a pronounced effect on the performance of the material. This new isorecticular structure produced 100 mL mg<sup>-1</sup> of CO under identical conditions. In addition to framework expansion, the catalyst performance was further tailored using a building-block heterogeneity approach. Since it was hypothesized that not all electroactive sites (cobalt porphyrin moieties) in the parent material fully participate in the reaction, owing to the low aqueous solubility of CO<sub>2</sub> (CO<sub>2</sub> is rate-limiting), a partial replacement of these sites with catalytically inactive copper porphyrin units was examined. Indeed, this catalyst dilution strategy led to materials that achieved TONs of up to 290,000, with an initial turnover frequency of 9,400 h<sup>-1</sup>. This corresponds to a 26-fold improvement in performance compared to the molecular cobalt complex employed for this reaction.

## Outlook

Although the focus of this Perspective was in considering reticular chemistry as the next generation of CO<sub>2</sub> reduction materials, it is important to point out that the economic feasibility of any CO<sub>2</sub> reduction system implemented on a grand scale remains a point of discussion among academics, economists and policymakers<sup>59</sup>. Be that as it may, when considering the next generation of CO<sub>2</sub> reduction systems, one has to take account of the advantages and drawbacks of both photo- and electrochemical processes. While photochemical reduction processes benefit from clean solar energy, they are currently hindered by the necessary evil of sacrificial donors as an electron source. This is even true in the case of MOFs. Thus far, MOFs have only been applied to one half of the catalytic process at a time and this must be addressed in order to develop more advanced Z scheme-like systems. Furthermore, as it stands now, a worthwhile photochemical reduction MOF catalyst requires a rather complex multicomponent system, which must take advantage of introducing photosensitizers to increase photonic and quantum efficiency, and catalytically active sites, and designing a SBU and/or linker with

the appropriate bandgap (photonic efficiency again). In this regard, a deeper fundamental understanding of the structure–chemistry–property relationship of these complex systems is essential prior to promoting the practicability of reticular chemistry for this purpose<sup>13</sup>. When turning attention to electrochemical reduction MOF/COF catalytic systems, the ideal overpotential can be determined experimentally such that the current and Faradaic efficiencies are optimized. This allows for the optimization of the MOF/COF catalyst in a way not possible with a photochemical approach, where not all of the absorbed photons can be utilized since they do not necessarily have the required potential to affect conversion or are limited by a fast charge carrier recombination with respect to the timescale of the reaction. As a consequence, the figures of merit for efficiency in electrocatalytic systems are considerably higher than those of their photocatalytic counterparts. By using reticular chemistry to design catalytic materials, the selectivity and activity criteria can be met for both photo- and electrochemical reduction processes. Hence, the determining factor for developing the next generation must lie in maximizing the efficiency. In this regard, electrochemical processes are far more advanced and represent a viable answer toward this end. It has been shown that electrocatalytically driven COF catalysts already meet all criteria for an active, selective and efficient reduction catalyst. The problem now lies not solely in materials design — although there are outstanding materials design challenges that remain (long-term catalytic recyclability and assessing other structure-function parameters for practical use) — but rather in implementing the electrocatalyst within the right system. Our view is that the next step in this progression is one in which a MOF/COF electrochemically reduces CO<sub>2</sub>, where the energy is derived from sunlight (Fig. 4). Such a photoelectrochemical approach combines the desired renewable energy input of photocatalytic systems with the higher efficiency of electrochemical reduction. The need for a sacrificial donor to feed electrons to the system is also removed as these electrons can be generated from water splitting on the counter electrode.

Received: 30 August 2017; Accepted: 25 January 2018;

Published online: 26 February 2018

## References

1. Concepcion, J. J., House, R. L., Papanikolas, J. M. & Meyer, T. J. *Proc. Natl Acad. Sci. USA* **109**, 15560–15564 (2012).
2. Liu, C., Colón, B. C., Ziesack, M., Silver, P. A. & Nocera, D. G. *Science* **352**, 1210–1213 (2016).
3. Sakimoto, K. K., Wong, A. B. & Yang, P. *Science* **351**, 74–77 (2016).
4. White, J. L. et al. *Chem. Rev.* **115**, 12888–12935 (2015).
5. Seh, Z. W. et al. *Science* **355**, eaad4998 (2017).
6. Chen, Y., Li, C. W. & Kanan, M. W. *J. Am. Chem. Soc.* **134**, 19969–19972 (2012).
7. Kim, D., Resasco, J., Yu, Y., Asiri, A. M. & Yang, P. *Nat. Commun.* **5**, 4948 (2014).
8. Cao, Z. et al. *J. Am. Chem. Soc.* **138**, 8120–8125 (2016).
9. Domen, K. & Hisatomi, T. *Faraday Discuss.* **198**, 11–35 (2017).
10. Morris, A. J., Meyer, G. J. & Fujita, E. *Acc. Chem. Res.* **42**, 1983–1994 (2009).
11. Costentin, C., Passard, G., Robert, M. & Savéant, J.-M. *Proc. Natl Acad. Sci. USA* **111**, 14990–14994 (2014).
12. Costentin, C., Drouet, S., Robert, M. & Savéant, J.-M. *Science* **338**, 90–94 (2012).
13. Rajeshwar, K., Thomas, A. & Janáky, C. *J. Phys. Chem. Lett.* **6**, 139–147 (2015).
14. Furukawa, H., Cordova, K. E., O’Keeffe, M. & Yaghi, O. M. *Science* **341**, 1230444 (2013).
15. Diercks, C. S. & Yaghi, O. M. *Science* **355**, eaal585 (2017).
16. Lee, J. et al. *Chem. Soc. Rev.* **38**, 1450–1459 (2009).
17. Zhang, T. & Lin, W. *Chem. Soc. Rev.* **43**, 5982–5993 (2014).
18. Farha, O. K. et al. *J. Am. Chem. Soc.* **134**, 15016–15021 (2012).
19. Deng, H. et al. *Science* **336**, 1018–1023 (2012).
20. Sun, L., Campbell, M. G. & Dincă, M. *Angew. Chem. Int. Ed.* **55**, 3566–3579 (2016).
21. Guo, J. et al. *Nat. Commun.* **4**, 2736 (2013).
22. Berardi, S. et al. *Chem. Soc. Rev.* **43**, 7501–7519 (2014).
23. Wang, C., Xie, Z., deKrafft, K. E. & Lin, W. *J. Am. Chem. Soc.* **133**, 13445–13454 (2011).

24. Hawecker, J., Lehn, J.-M. & Ziessel, R. *Helv. Chim. Acta* **69**, 1990–2012 (1986).
25. Keith, J. A., Grice, K. A., Kubiak, C. P. & Carter, E. A. *J. Am. Chem. Soc.* **135**, 15823–15829 (2013).
26. Ryu, U. J. et al. *Sci. Rep.* **7**, 612 (2017).
27. Wang, D., Huang, R., Liu, W., Sun, D. & Li, Z. *ACS Catal.* **4**, 4254–4260 (2014).
28. Whitfield, T. R., Wang, X., Liu, L. & Jacobson, A. J. *Solid State Sci.* **7**, 1096–1103 (2005).
29. Surlblé, S., Serre, C., Mellot-Draznieks, C., Millangea, F. & Férey, G. *Chem. Commun.* **0**, 284–286 (2008).
30. Chen, D., Xing, H., Wang, C. & Su, Z. *J. Mater. Chem. A* **4**, 2657–2662 (2016).
31. Doan, T. L. H. et al. *Chem. Asian J.* **10**, 2660–2668 (2015).
32. Nasalevich, M. A. et al. *Sci. Rep.* **6**, 23676 (2016).
33. Dan-Hardi, M. et al. *J. Am. Chem. Soc.* **131**, 10857–10859 (2009).
34. Fu, Y. et al. *Angew. Chem. Int. Ed.* **124**, 3420–3423 (2012).
35. Hendon, C. H. et al. *J. Am. Chem. Soc.* **135**, 10942–10945 (2013).
36. Logan, M. W. et al. *J. Mater. Chem. A* **5**, 11854–11863 (2017).
37. Khaletskaya, K. et al. *Chem. Mater.* **27**, 7248–7257 (2015).
38. Li, R. et al. *Adv. Mater.* **26**, 4783–4788 (2014).
39. Choi, K. M. et al. *J. Am. Chem. Soc.* **139**, 356–362 (2017).
40. Fei, H., Sampson, M. D., Lee, Y., Kubiak, C. P. & Cohen, S. M. *Inorg. Chem.* **54**, 6821–6828 (2015).
41. Riplinger, C., Sampson, M. D., Ritzmann, A. M., Kubiak, C. P. & Carter, E. A. *J. Am. Chem. Soc.* **136**, 16285–16298 (2014).
42. Lee, Y., Kim, S., Kang, J. K. & Cohen, S. M. *Chem. Commun.* **51**, 5735–5738 (2015).
43. Darago, L. E., Aubrey, M. L., Yu, C. J., Gonzalez, M. I. & Long, J. R. *J. Am. Chem. Soc.* **137**, 15703–15711 (2015).
44. Clough, A. J. et al. *J. Am. Chem. Soc.* **139**, 10863–10867 (2017).
45. Sheberla, D. et al. *J. Am. Chem. Soc.* **136**, 8859–8862 (2014).
46. Sun, L. et al. *Chem. Sci.* **8**, 4450–4457 (2017).
47. Janssen, R. A. J. & Nelson, J. *Adv. Mater.* **25**, 1847–1858 (2013).
48. Hendon, C. H., Rieth, A. J., Korzynski, M. D. & Dinca, M. *ACS Cent. Sci.* **3**, 554–563 (2017).
49. Trickett, C. A. et al. *Nat. Rev. Mater.* **2**, 17045 (2017).
50. Xiao, D. J. et al. *Nat. Chem.* **6**, 590–595 (2014).
51. Metzger, E. D., Comito, R. J., Hendon, C. H. & Dincă, M. *J. Am. Chem. Soc.* **139**, 757–762 (2017).
52. Costentin, C., Robert, M. & Savéant, J.-M. *Chem. Soc. Rev.* **42**, 2423–2436 (2013).
53. Morris, W. et al. *Inorg. Chem.* **51**, 6443–6445 (2012).
54. Hod, I. et al. *ACS Catal.* **5**, 6302–6309 (2015).
55. Fateeva, A. et al. *Angew. Chem. Int. Ed.* **51**, 7440–7444 (2012).
56. Kornienko, N. et al. *J. Am. Chem. Soc.* **137**, 14129–14135 (2015).
57. Wan, S. et al. *Chem. Mater.* **23**, 4094–4097 (2011).
58. Lin, S. et al. *Science* **349**, 1208–1213 (2015).
59. Mac Dowell, N., Fennell, P. S., Shah, N. & Maitland, G. C. *Nat. Clim. Change* **7**, 243–249 (2017).

## Acknowledgements

We would like to acknowledge Saudi Aramco (ORCP2390) for their continued collaboration and support. C.S.D. would like to acknowledge the Kavli Foundation for support through the Kavli Energy NanoScience Institute Philomathia graduate student fellowship. Y.L. is supported by the graduate student fellowship in the environmental sciences provided by the Philomathia Center. K.E.C. is grateful for discussions with A. Jamal (Saudi Aramco) during the preliminary stages of this manuscript. Finally, we acknowledge M. Prevot (UC Berkeley) for helpful discussions.

## Author contributions

K.E.C. and O.M.Y. conceived the general idea behind this Perspective. C.S.D. and K.E.C. wrote the manuscript under the mentorship of O.M.Y. Y.L. aided in figure creation. The manuscript was written through contributions of all authors. All authors have given approval to the final version of the manuscript.

## Competing interests

The authors declare no competing interests.

## Additional information

Reprints and permissions information is available at [www.nature.com/reprints](http://www.nature.com/reprints).

Correspondence and requests for materials should be addressed to O.M.Y.

**Publisher's note:** Springer Nature remains neutral with regard to jurisdictional claims in published maps and institutional affiliations.